J. Phys. Chem. A **1998,** *102,* 10113−10119 **10113**

Vibronic Interactions in Silicon Polyhedra of the Si_{46} Clathrate Compound

Kazunari Yoshizawa,* Takashi Kato, and Masamitsu Tachibana

Department of Molecular Engineering, Kyoto University, Sakyo-ku, Kyoto 606-8501, Japan

Tokio Yamabe

Department of Molecular Engineering, Kyoto University, Sakyo-ku, Kyoto 606-8501, Japan, and Institute for Fundamental Chemistry, 34-4 Takano-Nishihiraki-cho, Sakyo-ku, Kyoto 606-8103, Japan

Received: May 5, 1998

The vibronic (vibrational−electronic) interactions in the Si_{46} clathrate compound are discussed using the highly symmetric $(SiH)_{20}$ and $(SiH)_{24}$ cluster models to look at a possible correlation between the Jahn−Teller effect and the superconductivity. The vibronic coupling constants for six H_g modes in the mono-, tri-, and pentaanions of $(SiH)_{20}$ and for twelve E_4 modes in the tri- and pentaanions of $(SiH)_{24}$ are calculated using the MNDO-PM3 method, one of the most reliable semiempirical molecular orbital methods, to know which mode of vibration plays a governing role in the Jahn−Teller distortions of these interesting hypothetical multianions. The lowest mode of about 100 cm^{-1} appears to significantly couple with their degenerate electronic states to exhibit a large coupling constant in both silicon clusters. This type of low-frequency mode is characteristic of nanosized molecular systems and would have relevance to acoustic phonon modes in the solid. If the Jahn−Teller distortions play a role in the appearance of the molecular superconductivity in the silicon clathrate compound as suggested in the fullerene A_3C_{60} complexes, the lowest mode of vibration in the Si_{20} moiety should have a significant effect on the interesting solid-state properties.

Introduction

Various silicon networks are prepared by thermal decomposition of Zintl-phase silicon as a building block.[1] Yamanaka et al.[2] have demonstrated that a silicon clathrate compound, $(Na,Ba)_xSi_{46}$, prepared from Zintl-phase NaSi and $BaSi_2$, exhibits superconductivity[3] at 4 K, the elemental composition of this silicon clathrate being $Na_{2.9}Ba_{4.5}Si_{46}$. The structure of silicon clathrate compounds is isomorphous with that of the well-known gas hydrates,[4] and $(Na,Ba)_xSi_{46}$ belongs to the type-I structure, in which the dodecahedral (12-hedral) cage cluster of Si_{20} and the tetradecahedral (14-hedral) cage cluster of Si_{24} are linked together while sharing their faces, to lead to the three-dimensional silicon network. The unit cell containing two 12-hedra and six 14-hedra is a simple cubic structure (consisting of 46 Si atoms) with a lattice constant of 10.26 Å for $Na_2Ba_6Si_{46}$. All the Si atoms are linked together through sp^3-type covalent bonds, the distances and the angles of which are approximately equal to those of the diamond-type silicon network. The structural, electronic, and vibrational properties of the Si_{46} clathrate have been extensively investigated.[5] The ideal elemental composition is $Na_2Ba_6Si_{46}$ in which an Na atom is located at the center of each 12-hedral cage cluster and a Ba atom at the center of each 14-hedral one, as indicated in **1**.

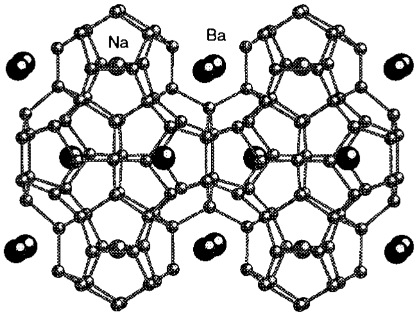

1

The $(K,Ba)_xSi_{46}$ and Ba_8Si_{46} compounds appeared later to also exhibit superconductivity at 4 and 8 K,[6] respectively, but neither Na_8Si_{46} nor Na_xSi_{136} shows superconductivity at a finite temperature.[7] It has been pointed out from band-structure calculations[8] and NMR measurements[9] that the Ba atoms play an important role in the appearance of superconductivity. It is well-known that Zintl-phase α-$ThSi_2$-type $SrSi_2$ and $CaSi_2$ and trigonal $BaSi_2$ compounds also exhibit superconductivity[10] and that diamond-type silicon is transformed into the β-Sn type structure and next into the simple-hexagonal structure under pressure to show superconductivity.[11] The $(Na,Ba)_xSi_{46}$ compound is the first example of a superconductor that consists of an sp^3 silicon network.

The structural features and interesting solid-state properties of the silicon clathrate compounds may have relevance to those of the fullerene A_3C_{60} complexes that exhibit high superconductive transition temperatures over 30 K, where A is an alkali metal such as Rb and Cs.[12] The LUMO (lowest unoccupied molecular orbital) of C_{60} is 3-fold degenerate (t_{1u}) due to its highly symmetric structure, and therefore the electronic state of the $C_{60}{}^{3-}$ trianion is 3-fold degenerate. So we expect that Jahn−Teller distortions should reasonably occur to lift the electronic degeneracy through coupling with certain modes of molecular vibration.[13,14] A large amount of theoretical work on the vibronic (vibrational−electronic) coupling and the Jahn−Teller effect of fullerene complexes has been conducted to account for the interesting solid-state phenomena of the A_3C_{60}

---

* To whom all correspondence should be addressed. E-mail: kazunari@scl.kyoto-u.ac.jp.

10.1021/jp982113z CCC: $15.00

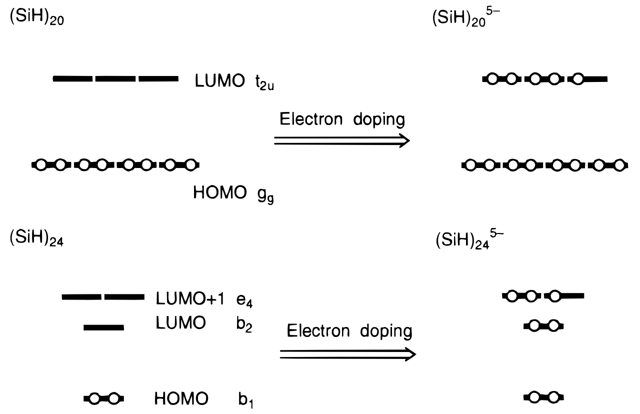

Figure 1. Energy levels of the HOMO and LUMO in $(SiH)_{20}$ and of the HOMO, LUMO, and (LUMO + 1) in $(SiH)_{24}$.

complexes.[15] We recently investigated the Jahn−Teller effect and possible superconductivity in negatively charged [18]-annulene, $(CH)_{18}$, which is an interesting molecular system with a highly symmetric D_{6h} geometry in the neutral state.[16] The low-frequency Jahn−Teller-active modes that cause distortions of the C−C framework of the molecule appeared to significantly couple with the degenerate electronic state to lead to large electron−phonon coupling constants in linear-chain models of the [18]annulene anions.

Since the $(Na,Ba)_xSi_{46}$ compound includes the highly symmetric Si_{20} and Si_{24} cage clusters which belong to the I_h and D_{6d} point groups, respectively, we expect that Jahn−Teller distortions should also occur in the anions of these silicon clusters. Note that Si_{20} and C_{60} belong to the same point group. In this article, we shed new light on a possible correlation between the Jahn−Teller effect in the Si_{20} and Si_{24} clusters and the superconductivity in the $(Na,Ba)_xSi_{46}$ compound. To calculate and analyze the vibronic coupling constants for the Jahn−Teller-active modes of vibration in these silicon clusters, we use the $(SiH)_{20}$ and $(SiH)_{24}$ models because, in contrast to the fullerene C_{60}, the Si_{20} and Si_{24} clusters themselves have a dangling bond (unpaired electron) at each Si atom, due to their strong sp^3 silicon nature. A cluster model, in which the electronic interactions within a small group of atoms are treated in detail, is an extreme way of looking at the electronic structure of solids. The cluster model and band theory provide us with complementary viewpoints, and applicability of these has been well established. The MNDO-PM3 (modified neglect of diatomic overlap, parametric method 3) method,[17] one of the most reliable semiempirical molecular orbital methods, was used for calculations of geometry optimization, vibrational analysis, and vibronic coupling constants.

Theory of Vibronic Interaction

We will use small letters for "one-electron levels" and capital letters for both "electronic" and "vibrational" states, as usual. The HOMO and LUMO of the $(SiH)_{20}$ cluster of the I_h symmetry are 4-fold (g_g) and 3-fold (t_{2u}) degenerate, respectively; both the HOMO and LUMO of the $(SiH)_{24}$ cluster of the D_{6d} symmetry are not degenerate, but the (LUMO + 1) is 2-fold (e_4) degenerate, as shown in Figure 1. We therefore expect that Jahn−Teller distortions should reasonably occur in the $(SiH)_{20}^{-}$, $(SiH)_{20}^{3-}$, $(SiH)_{20}^{5-}$, $(SiH)_{24}^{3-}$, and $(SiH)_{24}^{5-}$ clusters. Since the formal charge of Si in the $Na_{2.9}Ba_{4.5}Si_{46}$ clathrate compound is −0.259, the formal charges of the Si_{20} and Si_{24} clusters are counted to be −5.17 and −6.21, respectively. Thus, the charge states we consider in this paper are quite reasonable if all Na and Ba atoms in the clathrate compound are almost completely ionized.

We consider the vibronic interactions in the two silicon cage models. The vibronic mixing matrix element,[18−21] $W_{\gamma'\gamma''}(r, Q)$, is given by

$$W_{\gamma'\gamma''}(r, Q) = V_{\gamma'\gamma''}(r, Q) - V_{\gamma'\gamma''}(r, 0) = \sum_{\alpha}\left(\frac{\partial V_{\gamma'\gamma''}}{\partial Q_{\alpha}}\right)_0 Q_{\alpha} + \frac{1}{2}\sum_{\alpha,\beta}\left(\frac{\partial^2 V_{\gamma'\gamma''}}{\partial Q_{\alpha}\,\partial Q_{\beta}}\right)_0 Q_{\alpha}Q_{\beta} \quad (1)$$

where $V_{\gamma'\gamma''}(r, Q)$ is defined as

$$V_{\gamma'\gamma''}(r, Q) = \langle \phi_{\gamma'}|V(r, Q)|\phi_{\gamma''}\rangle \quad (2)$$

$V(r, Q)$ includes the electron−nucleus and nucleus−nucleus interactions, and $\phi_{\gamma'}$ and $\phi_{\gamma''}$ are electronic wave functions. r and Q signify the whole set of coordinates of the electrons and nuclei, respectively. The first term on the right-hand side of eq 1 corresponds to the linear vibronic coupling constant. In the second term on the right-hand side, there are diagonal matrix elements of vibronic interactions, i.e., force constants. Now we take two approximations into account. First we ignore the nondiagonal matrix elements containing the quadratic vibronic constants; only terms of type Q_{α}^2 are taken into account. Second we focus upon the diagonal processes that can couple the electrons belonging to the same irreducible representations; thus, we consider both the electronic states γ' and γ'' that belong to the T_{2u} state in $(SiH)_{20}$ and the E_4 state in $(SiH)_{24}$. The direct product of the T_{2u} state of the mono-, tri-, and pentaanions of $(SiH)_{20}$ and that of the E_4 state of the tri- and pentaanions of $(SiH)_{24}$ can be reduced as

$$T_{2u} \times T_{2u} = A_g + T_{2g} + H_g \quad (3a)$$

and

$$E_4 \times E_4 = A_1 + A_2 + E_4 \quad (3b)$$

respectively. Thus, the 5-fold degenerate H_g modes of vibration lift the 3-fold degenerate electronic states of the $(SiH)_{20}^{-}$, $(SiH)_{20}^{3-}$, and $(SiH)_{20}^{5-}$ clusters, and the 2-fold degenerate E_4 modes of vibration lift the 2-fold degenerate electronic states of the $(SiH)_{24}^{3-}$ and $(SiH)_{24}^{5-}$ clusters. The number of such H_g modes is 6 for $(SiH)_{20}$, and that of such E_4 modes is 12 for $(SiH)_{24}$. We therefore have to consider the multimode problems, in which there are more than one set of Jahn−Teller active modes of given symmetry, according to Bersuker.[20] However, in the limit of linear vibronic coupling, one can treat each Jahn−Teller-active mode independently.

Vibronic Coupling in the $(SiH)_{24}$ Anions. Let us first consider the vibronic coupling and the Jahn−Teller effect on the anions of $(SiH)_{24}$. These are simple $E_4 \times E_4$ Jahn−Teller systems. The two sheets of the adiabatic potential $U^{(E_4)}_{m\gamma'\gamma''}(Q_{E_4\theta m}, Q_{E_4\epsilon m})$ of the 2-fold degenerate electronic state that couples with the mth vibrational mode of the anions of $(SiH)_{24}$ are given in the form of eq 4, where $Q_{E_4\gamma m}$ is the vibrational normal coordinate belonging to row γ of the mth vibrational mode of the irreducible representation E_4. Here γ takes two vibrational states θ and ϵ. The first term on the right-hand side of eq 4 is the elastic term, and $\langle E_{4\gamma'}|(\partial V/\partial Q_{E_4\gamma m})_0|E_{4\gamma''}\rangle$ in the second term corresponds to the linear vibronic coupling constant, which is a measure of the interaction between the vibration labeled by γ

$$U^{(E_4)}_{m\gamma'\gamma''}(Q_{E_4\theta m}, Q_{E_4\epsilon m}) = \frac{1}{2}\sum_{\gamma=\theta,\epsilon} K_{E_4 m} Q_{E_4\gamma m}{}^2 + \sum_{\gamma=\theta,\epsilon}\left\langle E_{4\gamma'}\left|\left(\frac{\partial V}{\partial Q_{E_4\gamma m}}\right)_0\right|E_{4\gamma''}\right\rangle Q_{E_4\gamma m} \quad (4)$$

$$m = 1, 2, ..., 12$$

in the *m*th mode and the electronic states labeled by γ' and γ'' in the irreducible representation E_4. According to the Wigner−Eckart theorem,[20,21] we can rewrite the second term on the right-hand side of eq 4 using the Clebsch−Gordan coefficients and we get the Jahn−Teller coupling matrix as

$$V_{E_4 m} = A_m \begin{pmatrix} -Q_{E_4\epsilon m} & Q_{E_4\theta m} \\ Q_{E_4\theta m} & Q_{E_4\epsilon m} \end{pmatrix} \quad (5)$$

where A_m is the vibronic coupling constant for the *m*th mode:

$$A_m = \frac{1}{2}\left\langle E_4 \left\| \left(\frac{\partial V}{\partial Q_{E_4 m}}\right)_0 \right\| E_4 \right\rangle \quad (6)$$

A_m depends only on the irreducible representation and not on the rows. From eq 5, eq 4 can be transformed into

$$U^{(E_4)}_m(Q_{E_4\theta m}, Q_{E_4\epsilon m}) = \frac{1}{2}K_{E_4 m}(Q_{E_4\theta m}{}^2 + Q_{E_4\epsilon m}{}^2)\begin{pmatrix} 1 & 0 \\ 0 & 1 \end{pmatrix} + A_m \begin{pmatrix} -Q_{E_4\epsilon m} & Q_{E_4\theta m} \\ Q_{E_4\theta m} & Q_{E_4\epsilon m} \end{pmatrix} \quad (7)$$

This can be easily diagonalized, and thus the adiabatic potentials in the *m*th vibrational mode of the $(SiH)_{24}$ anionic clusters become

$$U^{(E_4)}_{m\pm}(Q_{E_4\theta m}, Q_{E_4\epsilon m}) = \frac{1}{2}K_{E_4 m}(Q_{E_4\theta m}{}^2 + Q_{E_4\epsilon m}{}^2) \pm A_m\sqrt{Q_{E_4\theta m}{}^2 + Q_{E_4\epsilon m}{}^2} \quad (8)$$

In a linear approximation, the adiabatic potential in each mode has the form of a rotation surface, the so-called Mexican hat. A cross section of the Mexican hat (for the Jahn−Teller distortion of the $(SiH)_{24}$ anions) cut by the plane $Q_{E_4\epsilon m} = 0$ is illustrated in Figure 2. According to the Jahn−Teller theorem,[13b] the D_{6d} structure of $(SiH)_{24}$ should be distorted into D_{2d} and S_4 structures through the E_4 modes of vibration. The dimensionless linear diagonal coupling constant, $g_{E_4 m}$, for the *m*th vibrational mode of negatively charged $(SiH)_{24}$ is defined by

$$g_{E_4 m} = \frac{1}{2\hbar\omega_m}\left\langle E_4 \left\| \left(\frac{\partial V}{\partial q_{E_4 m}}\right)_0 \right\| E_4 \right\rangle \quad (9)$$

In this equation, $q_{E_4 m}$ is the dimensionless normal coordinate[22] defined as

$$q_{E_4 m} = (\omega_m/\hbar)^{1/2} Q_{E_4 m} \quad (10)$$

Vibronic Coupling in the $(SiH)_{20}$ Anions. Let us next describe the vibronic coupling and the Jahn−Teller effect on the anions of $(SiH)_{20}$. These are the $T_{2u} \times H_g$ Jahn−Teller system studied by Kholpin, Polinger, and Bersuker;[23] the problem is a little complicated compared with the $(SiH)_{24}$ cluster. The Jahn−Teller coupling matrix in $(SiH)_{20}$ is defined as

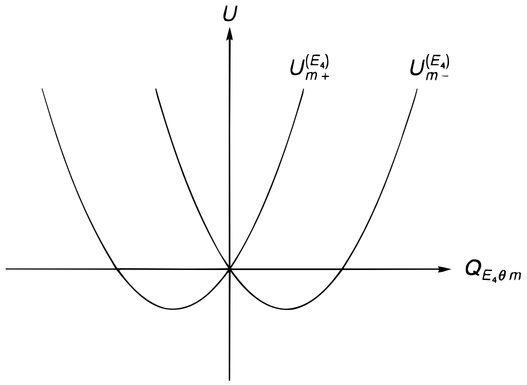

Figure 2. Jahn−Teller distortions for $(SiH)_{24}$ in the *m*th vibrational mode.

$$V_{H_g m} = \frac{I_m}{\sqrt{3}}\begin{pmatrix} -Q_{H_g\theta m} + \sqrt{3}Q_{H_g\epsilon m} & 0 & 0 \\ 0 & -Q_{H_g\theta m} - \sqrt{3}Q_{H_g\epsilon m} & 0 \\ 0 & 0 & 2Q_{H_g\theta m} \end{pmatrix} + I_m\begin{pmatrix} 0 & Q_{H_g\zeta m} & Q_{H_g\eta m} \\ Q_{H_g\zeta m} & 0 & Q_{H_g\xi m} \\ Q_{H_g\eta m} & Q_{H_g\xi m} & 0 \end{pmatrix} \quad (11)$$

$$m = 1, 2, ..., 6$$

where I_m is the vibronic coupling constant for the *m*th mode of vibration defined as

$$I_m = \left\langle T_{2u} \left\| \left(\frac{\partial V}{\partial Q_{H_g m}}\right)_0 \right\| T_{2u} \right\rangle \quad (12)$$

Considering the elastic terms, the adiabatic potential becomes

$$U^{(H_g)}_m(Q_{H_g\theta m}, Q_{H_g\epsilon m}, Q_{H_g\xi m}, Q_{H_g\eta m}, Q_{H_g\zeta m}) = \frac{1}{2}K_{H_g m}(Q_{H_g\theta m}{}^2 + Q_{H_g\epsilon m}{}^2 + Q_{H_g\xi m}{}^2 + Q_{H_g\eta m}{}^2 + Q_{H_g\zeta m}{}^2)\begin{pmatrix} 1 & 0 & 0 \\ 0 & 1 & 0 \\ 0 & 0 & 1 \end{pmatrix} + \frac{I_m}{\sqrt{3}}\begin{pmatrix} -Q_{H_g\theta m} + \sqrt{3}Q_{H_g\epsilon m} & 0 & 0 \\ 0 & -Q_{H_g\theta m} - \sqrt{3}Q_{H_g\epsilon m} & 0 \\ 0 & 0 & 2Q_{H_g\theta m} \end{pmatrix} + I_m\begin{pmatrix} 0 & Q_{H_g\zeta m} & Q_{H_g\eta m} \\ Q_{H_g\zeta m} & 0 & Q_{H_g\xi m} \\ Q_{H_g\eta m} & Q_{H_g\xi m} & 0 \end{pmatrix} \quad (13)$$

Now we consider only one mode. For example, when we consider only the $Q_{H_g\zeta m}$ mode ($Q_{H_g\theta m} = Q_{H_g\epsilon m} = Q_{H_g\xi m} = Q_{H_g\eta m} = 0$), the adiabatic potentials in row ζ of the *m*th mode of negatively charged $(SiH)_{20}$ become

$$U^{(H_g)}_m(Q_{H_g\zeta m}) = \frac{1}{2}K_{H_g m}Q_{H_g\zeta m}{}^2\begin{pmatrix} 1 & 0 & 0 \\ 0 & 1 & 0 \\ 0 & 0 & 1 \end{pmatrix} + I_m\begin{pmatrix} 0 & Q_{H_g\zeta m} & 0 \\ Q_{H_g\zeta m} & 0 & 0 \\ 0 & 0 & 0 \end{pmatrix} \quad (14)$$

This can be easily diagonalized, and thus, the adiabatic potentials in row ζ of the *m*th mode of negatively charged $(SiH)_{20}$ cut by the plane $Q_{\mathrm{H_g}\theta m} = Q_{\mathrm{H_g}\epsilon m} = Q_{\mathrm{H_g}\xi m} = Q_{\mathrm{H_g}\eta m} = 0$ become

$$U_{m0}^{(\mathrm{H_g})}(Q_{\mathrm{H_g}\zeta m}) = \frac{1}{2}K_{\mathrm{H_g}m}{Q_{\mathrm{H_g}\zeta m}}^2 \tag{15a}$$

$$U_{m\pm}^{(\mathrm{H_g})}(Q_{\mathrm{H_g}\zeta m}) = \frac{1}{2}K_{\mathrm{H_g}m}{Q_{\mathrm{H_g}\zeta m}}^2 \pm I_m Q_{\mathrm{H_g}\zeta m} \tag{15b}$$

$$Q_{\mathrm{H_g}\theta m} = Q_{\mathrm{H_g}\epsilon m} = Q_{\mathrm{H_g}\xi m} = Q_{\mathrm{H_g}\eta m} = 0$$

In a similar way, the adiabatic potential in rows ϵ, ξ, and η of the mth mode can be expressed by the same equations as that in row ζ. Thus, we can summarize the adiabatic potential as follows:

$$U_{m0}^{(\mathrm{H_g})}(Q_{\mathrm{H_g}\gamma m}) = \frac{1}{2}K_{\mathrm{H_g}m}{Q_{\mathrm{H_g}\gamma m}}^2 \tag{16a}$$

$$U_{m\pm}^{(\mathrm{H_g})}(Q_{\mathrm{H_g}\gamma m}) = \frac{1}{2}K_{\mathrm{H_g}m}{Q_{\mathrm{H_g}\gamma m}}^2 \pm I_m Q_{\mathrm{H_g}\gamma m} \tag{16b}$$

$$\gamma = \epsilon, \xi, \eta, \zeta$$

$$Q_{\mathrm{H_g}\gamma' m} = 0 \ (\gamma' \neq \gamma)$$

These potential curves are illustrated in Figure 3.

When we consider only the $Q_{\mathrm{H_g}\theta m}$ mode ($Q_{\mathrm{H_g}\epsilon m} = Q_{\mathrm{H_g}\xi m} = Q_{\mathrm{H_g}\eta m} = Q_{\mathrm{H_g}\zeta m} = 0$), the adiabatic potential in row θ of the mth mode of negatively charged $(\mathrm{SiH})_{20}$ cut by the plane $Q_{\mathrm{H_g}\epsilon m} = Q_{\mathrm{H_g}\xi m} = Q_{\mathrm{H_g}\eta m} = Q_{\mathrm{H_g}\zeta m} = 0$ becomes

$$U_m^{(\mathrm{H_g})}(Q_{\mathrm{H_g}\theta m}) = \frac{1}{2}K_{\mathrm{H_g}m}{Q_{\mathrm{H_g}\theta m}}^2 \begin{pmatrix} 1 & 0 & 0 \\ 0 & 1 & 0 \\ 0 & 0 & 1 \end{pmatrix} + \frac{I_m}{\sqrt{3}} \begin{pmatrix} -Q_{\mathrm{H_g}\theta m} & 0 & 0 \\ 0 & -Q_{\mathrm{H_g}\theta m} & 0 \\ 0 & 0 & 2Q_{\mathrm{H_g}\theta m} \end{pmatrix} \tag{17}$$

This has been already diagonalized, and thus, the adiabatic potentials in row θ of the mth mode of negatively charged $(\mathrm{SiH})_{20}$ cut by the plane $Q_{\mathrm{H_g}\epsilon m} = Q_{\mathrm{H_g}\xi m} = Q_{\mathrm{H_g}\eta m} = Q_{\mathrm{H_g}\zeta m} = 0$ become

$$U_{m1}^{(\mathrm{H_g})}(Q_{\mathrm{H_g}\theta m}) = \frac{1}{2}K_{\mathrm{H_g}m}{Q_{\mathrm{H_g}\theta m}}^2 - \frac{I_m}{\sqrt{3}}Q_{\mathrm{H_g}\theta m} \tag{18a}$$

$$U_{m2}^{(\mathrm{H_g})}(Q_{\mathrm{H_g}\theta m}) = \frac{1}{2}K_{\mathrm{H_g}m}{Q_{\mathrm{H_g}\theta m}}^2 + \frac{2I_m}{\sqrt{3}}Q_{\mathrm{H_g}\theta m} \tag{18b}$$

$$Q_{\mathrm{H_g}\epsilon m} = Q_{\mathrm{H_g}\xi m} = Q_{\mathrm{H_g}\eta m} = Q_{\mathrm{H_g}\zeta m} = 0$$

This potential curve is illustrated in Figure 3. The Jahn−Teller theorem[13b] predicts that the I_h structure of $(\mathrm{SiH})_{20}$ should be distorted into D_{5d}, D_{3d}, D_{2h}, and C_{2h} structures through $\mathrm{H_g}$ modes of vibration. The dimensionless linear diagonal coupling constant for the mth vibrational mode of the $(\mathrm{SiH})_{20}$ anions is defined by

$$g_{\mathrm{H_g}m} = \frac{1}{\hbar\omega_m}\left\langle \mathrm{T_{2u}} \middle\| \left(\frac{\partial V}{\partial q_{\mathrm{H_g}m}}\right)_0 \middle\| \mathrm{T_{2u}} \right\rangle \tag{19}$$

In this equation, $q_{\mathrm{H_g}m}$ is the dimensionless normal coordinate[22] defined as

$$q_{\mathrm{H_g}m} = (\omega_m/\hbar)^{1/2} Q_{\mathrm{H_g}m} \tag{20}$$

Results and Discussion

Molecular orbital calculations and vibrational analyses were carried out using the MNDO-PM3 method,[17] implemented with the Gaussian 94 program.[24] This method is one of the most reliable semiempirical molecular orbital methods, especially for bond length, heat of formation, and ionization potential. The optimized structures of the neutral $(\mathrm{SiH})_{20}$ and $(\mathrm{SiH})_{24}$ clusters are shown in Figure 4. These neutral structures were confirmed to be a minimum on each potential energy surface from vibrational analyses. The Si−Si bond distances of approximately 2.36 Å and the bond angles of approximately 108° are consistent with those of the diamond-type silicon network, except for the angle of 120° in the hexagon of $(\mathrm{SiH})_{24}$.

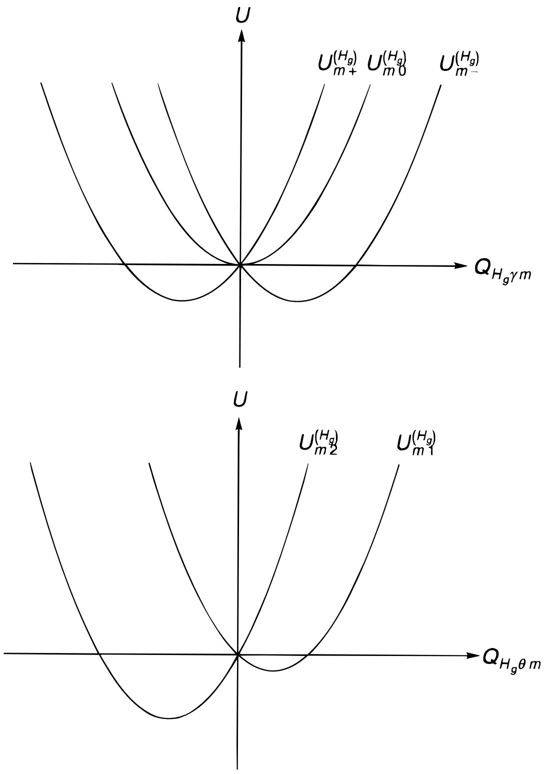

Figure 3. Jahn−Teller distortions for $(\mathrm{SiH})_{20}$ in the mth vibrational mode.

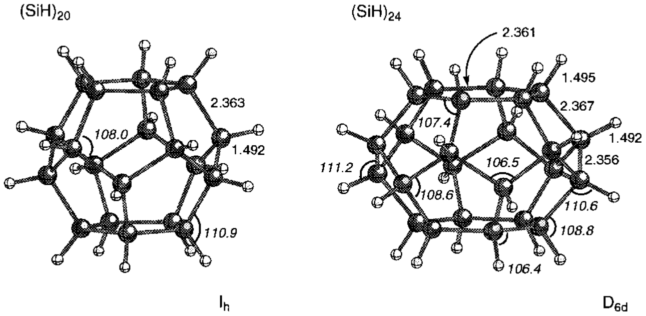

Figure 4. Optimized I_h and D_{6d} structures of $(\mathrm{SiH})_{20}$ and $(\mathrm{SiH})_{24}$, respectively, at the PM3 level.

The 5-fold degenerate $\mathrm{H_g}$ modes of vibration for the $(\mathrm{SiH})_{20}$ cluster are shown in Figure 5; we indicate here only one of each $\mathrm{H_g}$ mode. These Jahn−Teller-active modes should remove the degenerate $\mathrm{T_{2u}}$ electronic states of the mono-, tri-, and pentaanions, as mentioned above. The low-frequency modes, ω_1 and ω_2, are ascribed to cage deformation of the $(\mathrm{SiH})_{20}$ cluster; the ω_3, ω_4, and ω_5 modes are ascribed to Si−Si stretching coupled with Si−H bending; the highest ω_6 mode is ascribed to Si−H stretching. These computed frequencies are consistent with general trends in reference values from infrared spectra[25] and the Raman spectra of the $\mathrm{Si_{46}}$ clathrate compounds,[26] but the computed Si−H frequency of 1895 cm^{-1} is

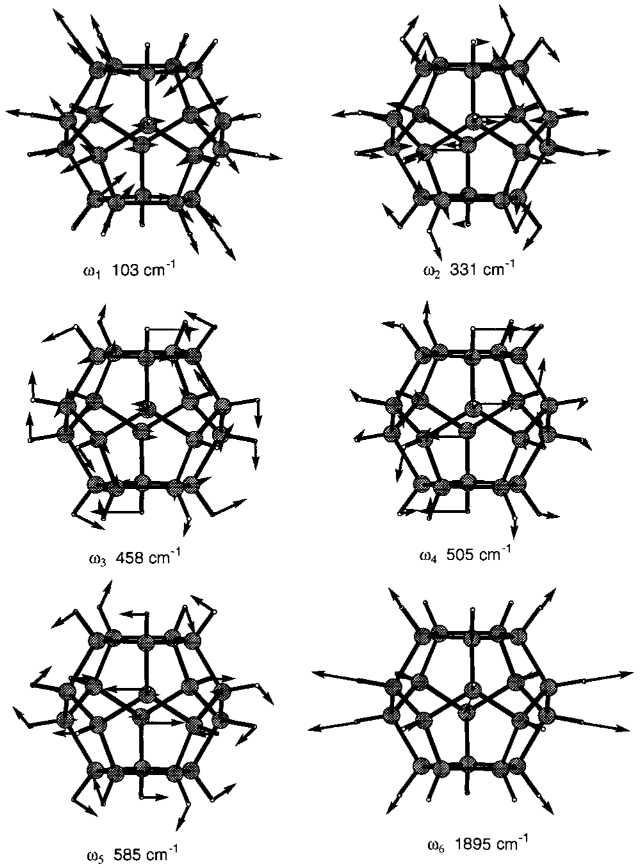

Figure 5. H_g vibrational modes of $(SiH)_{20}$.

TABLE 1: Vibronic Coupling Constants, $g_{H_g m}$, for the $(SiH)_{20}^-$, $(SiH)_{20}^{3-}$, and $(SiH)_{20}^{5-}$ Cage Clusters

	mode (cm^{-1})					
	ω_1 (103)	ω_2 (331)	ω_3 (458)	ω_4 (505)	ω_5 (585)	ω_6 (1895)
$(SiH)_{20}^-$	20.23	0.75	0.25	0.19	0.38	0.31
$(SiH)_{20}^{3-}$	17.22	2.83	2.20	2.01	1.45	0.19
$(SiH)_{20}^{5-}$	3.90	1.01	0.75	0.25	0.44	0.06

smaller than reference Si−H stretching values lying in a range of 2100−2250 cm^{-1}. The MNDO-PM3 method has a tendency to systematically underestimate Si−H stretching values of silicon compounds.[27]

We next consider the vibronic coupling constants for the mono-, tri-, and pentaanions of the $(SiH)_{20}$ cluster. In these charge states the highly symmetric I_h structure is unstable and leads to distorted structures in order to remove the electronic degeneracies according to the Jahn−Teller theorem.[13] In Table 1 we list the computed vibronic coupling constants, $g_{H_g m}$, of the $(SiH)_{20}^-$, $(SiH)_{20}^{3-}$, and $(SiH)_{20}^{5-}$ clusters for the six H_g modes. These values correspond to the derivatives of the total energy at the original point, obtained by distorting the equilibrium structure of the molecule along an H_g vibrational normal coordinate indicated in Figure 5. The lowest mode, ω_1, of 103 cm^{-1}, which is similar to the acoustic phonon mode in the solid because it is responsible for a cage deformation of the $(SiH)_{20}$ cluster, has the largest vibronic coupling constant in these anionic clusters. This type of vibration can be seen in nanosized molecular systems such as [18]annulene and coronene[28] but not in small molecules such as benzene. Thus, the lowest mode of vibration appears to greatly contribute to the Jahn−Teller distortion of the anions of the $(SiH)_{20}$ cluster.

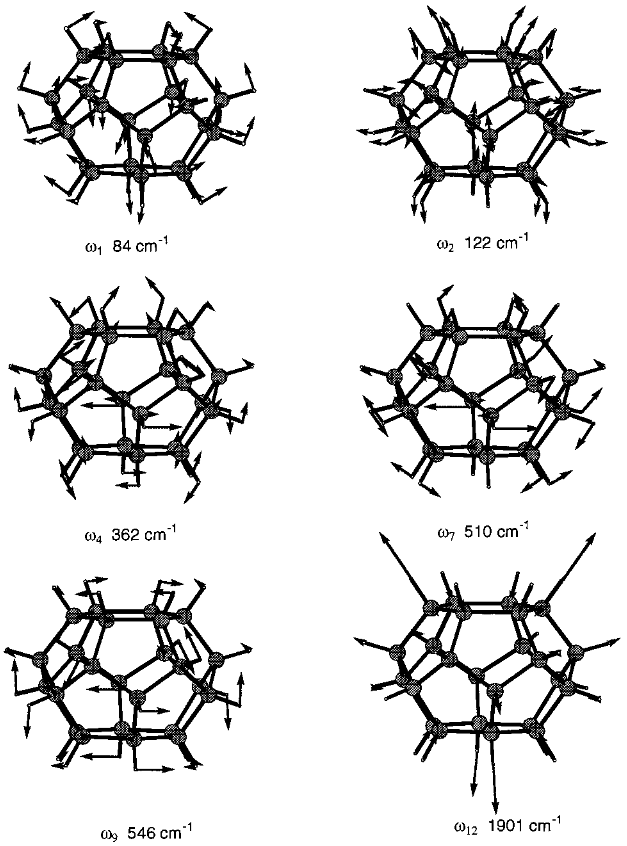

Figure 6. Selected E_4 vibrational modes of $(SiH)_{24}$.

Having described the vibronic coupling constants of the $(SiH)_{20}$ anions, we next turn our attention to the vibrational modes and coupling constants of the $(SiH)_{24}$ anions. Selected E_4 modes of vibration for the $(SiH)_{24}$ cluster are shown in Figure 6. These are also classified into cage deformation of the cluster (ω_1 and ω_2), Si−Si stretching coupled with Si−H bending (ω_4, ω_7, and ω_9), and Si−H stretching (ω_{12}).

The computed coupling constants, $g_{E_4 m}$, of the $(SiH)_{24}^{3-}$ and $(SiH)_{24}^{5-}$ clusters for the twelve E_4 modes of vibration are listed in Table 2. These values appear to be small compared with those of the $(SiH)_{20}$ anionic clusters listed in Table 1; we thus find that the electron−vibration coupling in the $(SiH)_{24}^{3-}$ and $(SiH)_{24}^{5-}$ clusters is not significant in contrast to that in the $(SiH)_{20}$ anionic clusters. Although the H_g and E_4 modes of vibration are Jahn−Teller active in the $(SiH)_{20}$ and $(SiH)_{24}$ anionic clusters, respectively, they behave in different ways in contributing to the electron−vibration coupling. But we can conclude in general that high-frequency modes, which derive mainly from hydrogen motions of the $(SiH)_{20}$ and $(SiH)_{24}$ clusters, have small coupling constants. Thus, such hydrogen motions do not significantly couple with the degenerate electronic states, and accordingly applicability of the hypothetical cluster models terminated by hydrogen atoms can be rationalized.

TABLE 2: Vibronic Coupling Constants, $g_{E_4 m}$, for the $(SiH)_{24}^{3-}$ and $(SiH)_{24}^{5-}$ Cage Clusters

	mode (cm^{-1})											
	ω_1 (84)	ω_2 (122)	ω_3 (191)	ω_4 (362)	ω_5 (432)	ω_6 (459)	ω_7 (510)	ω_8 (543)	ω_9 (546)	ω_{10} (582)	ω_{11} (1894)	ω_{12} (1901)
$(SiH)_{24}^{3-}$	1.95	0.38	0.19	0.25	0.06	0.06	0.19	0.06	0.19	0.00	0.00	0.00
$(SiH)_{24}^{5-}$	0.06	0.00	0.13	0.00	0.00	0.00	0.00	0.00	0.00	0.00	0.00	0.00

On the basis of the vibronic coupling constants for the $(SiH)_{20}$ and $(SiH)_{24}$ anionic clusters, let us consider a possible correlation between the Jahn−Teller effect and the superconductivity of the $(Na,Ba)_xSi_{46}$ clathrate compound. As mentioned above, the charge states we have considered are quite realistic from formal electron counting so that it is rational that we assume that the Jahn−Teller distortions of the Si_{20} and Si_{24} cage clusters will play an important role in the solid-state properties of the $(Na,Ba)_xSi_{46}$ clathrate compound. From an analogy with the fullerene A_3C_{60}, we think that the Jahn−Teller distortion of the Si_{20} moiety should contribute to the appearance of superconductivity in the $(Na,Ba)_xSi_{46}$ clathrate compound because the vibronic coupling constants for the $(SiH)_{20}$ anionic cluster are much larger than those for the $(SiH)_{24}$ anionic cluster.

$(SiH)_{20}$ and $(SiH)_{24}$ are, of course, our cluster models for the $(Na,Ba)_xSi_{46}$, Ba_8Si_{46}, and Na_8Si_{46} clathrate compounds. But it is difficult to find a good reason to account for superconductivity in the first two solids but no superconductivity in the third one. One can see a similar situation for the fullerene A_3C_{60} complexes, in which superconductivity appears in K_3C_{60} and Rb_3C_{60} but not in Na_3C_{60}.[12] One of the clues to understanding the superconductivity of A_3C_{60} has been proposed to come from the dependence of the superconducting transition temperatures T_c on lattice parameters.[29] Larger intercalant ions cause lattice expansion and a corresponding increase in T_c. Similarly, increasing the pressure on a sample reduces the lattice spacing and concomitantly the T_c. Since the lattice parameter determines the magnitude of the density of states at the Fermi level, the lattice parameter is the key to understanding the interesting solid-state properties of the A_3C_{60} complexes and the Si_{46} clathrate compounds. In fact, according to refs 2c and 6b, the lattice constants for the Na_8Si_{46}, $Na_2Ba_6Si_{46}$, and Ba_8Si_{46} compounds are 10.19, 10.26, and 10.33 Å, respectively. T_c increases with an increase in lattice constant if we consider the T_c of Na_8Si_{46} to be 0 K.

As mentioned earlier in this article, band-structure calculations[8] suggested that the Ba atoms in **1** play an important role in the superconductivity of the $(Na,Ba)_xSi_{46}$ clathrate compound. The Ba 5d bands are calculated to lie just at the Fermi level of the nondoped Si_{46} clathrate, resulting in an increase in the density of states at the Fermi level. Such an increase in the density of states would significantly contribute to the appearance of superconductivity. Moreover, NMR measurements[9,30] demonstrated that the Ba and Na atoms are partially ionized in contrast to the fullerene A_3C_{60} complexes, in which alkali metals are nearly completely ionized. If we follow the NMR result, the mono- or trianions for the Si_{20} and Si_{24} clusters may be realistic charge states. The computed phonon density of states for the Si_{46} clathrate is classified into two 100−200 and 300−550 cm^{-1} spectra,[5b,c] being qualitatively consistent with our vibrational analyses for the isolated $(SiH)_{20}$ and $(SiH)_{24}$ clusters, of course, except for the Si−H stretching modes of the model clusters. We showed in Table 1 that the lowest H_g mode of vibration affords a very large coupling constant in the $(SiH)_{20}^-$ and $(SiH)_{20}^{3-}$ clusters; thus the Si_{20} cluster would have relevance to the superconductivity rather than the Si_{24} one if the Jahn−Teller distortions play an essential role in the $(Na,Ba)_xSi_{46}$ clathrate compound, as suggested for the A_3C_{60} complexes.

Concluding Remarks

We have studied the vibronic interactions in the Si_{46} clathrate compound using the highly symmetric $(SiH)_{20}$ and $(SiH)_{24}$ cluster models to look at a possible correlation between the Jahn−Teller effect and the molecular superconductivity. The vibronic coupling constants for six H_g modes in the mono-, tri-, and pentaanions of $(SiH)_{20}$ and for twelve E_4 modes in the tri- and pentaanions of $(SiH)_{24}$ were calculated in order to know which vibrational mode plays an essential role in the Jahn−Teller distortions of these multianions, interesting degenerate molecular systems. The lowest modes of about 100 cm^{-1} in the spectra of the two clusters appear to significantly couple with their degenerate electronic states to lead to much greater coupling constants for both silicon clusters. In particular, the H_g mode of 103 cm^{-1} for the $(SiH)_{20}$ cluster has the largest coupling constant for each anion. This type of low-frequency mode is characteristic of nanosized molecular systems and has relevance to the acoustic phonon mode in the solid. If the Jahn−Teller distortions play a role in the appearance of molecular superconductivity in the silicon clathrate compound as in the fullerene A_3C_{60} complexes, the lowest mode of vibration for the Si_{20} moiety should have a significant effect on the interesting solid-state properties.

Acknowledgment. We are grateful for a Grant-in-Aid for Scientific Research on the Priority Area "The Chemistry of Interelement Linkage" from the Ministry of Education, Science, Sports and Culture of Japan and to the "Research for the Future" Program from the Japan Society for the Promotion of Science (JSPS-RFTF96P00206) for their support of this work. T.K. is grateful for Research Fellowships from the JSPS for Young Scientists. Computations were partly carried out at the Supercomputer Laboratory of Kyoto University and at the Computer Center of the Institute for Molecular Science.

References and Notes

(1) (a) Cros, C.; Pouchard, M.; Hagenmuller, E. P. *J. Solid State Chem.* **1970**, *2*, 570. (b) Cordier, G.; Woll, P. *J. Less-Common Met.* **1991**, *169*, 291. (c) Yamanaka, S.; Matsu-ura, H.; Ishikawa, M. *Mater. Res. Bull.* **1996**, *31*, 307.

(2) (a) Kawaji, H.; Horie, H.; Yamanaka, S.; Ishikawa, M. *Phys. Rev. Lett.* **1995**, *74*, 1427. (b) Yamanaka, S.; Horie, H.; Nakano, H.; Ishikawa, M. *Fullerene Sci. Technol*. **1995**, *3*, 21. (c) Yamanaka, S.; Kawaji, H.; Ishikawa, M. *Mater. Sci. Forum* **1996**, *232*, 103. (d) Kawaji, H.; Iwai, K.; Yamanaka, S.; Ishikawa, M. *Solid State Commun*. **1996**, *100*, 393.

(3) For example: (a) Kittel, C. *Quantum Theory of Solids*; Wiley: New York, 1963. (b) Schrieffer, J. R. *Theory of Superconductivity*; Addison-Wesley: Reading, MA, 1964. (c) de Gennes, P. G. *Superconductivity of Metals and Alloys*; Benjamin: New York, 1966. (d) Ziman, J. M. *Principles of the Theory of Solids*; Cambridge University Press: Cambridge, U.K., 1972. (e) Ibach, H.; Lüth, H. *Solid-State Physics*; Springer: Berlin, 1995.

(4) (a) Claussen, W. F. *J. Chem. Phys*. **1951**, *19*, 259. (b) StackelBerg, M. V.; Müller, H. R. *J. Chem. Phys*. **1951**, *19*, 1319. (c) Claussen, W. F. *J. Chem. Phys.* **1951**, *19*, 1425. (d) Kasper, J. S.; Hagenmuller, P.; Pouchard, M.; Cros, C. *Science* **1965**, *150*, 1713.

(5) (a) Adams, G. B.; O'Keeffe, M.; Demkov, A. A.; Sankey, O. F.; Huang, Y.-M. *Phys. Rev. B* **1994**, *49*, 8048. (b) Menon, M.; Richter, E.; Subbaswamy, K. R. *Phys. Rev. B* **1997**, *56*, 12290. (c) Kahn, D.; Lu, J. P. *Phys. Rev. B* **1997**, *56*, 13898.

(6) (a) Yamanaka, S.; Horie, H.; Kawaji, H.; Ishikawa, M. *Eur. J. Solid State Inorg. Chem*. **1995**, *32*, 799. (b) Yamanaka, S.; Enishi, E.; Yasukawa, M.; Fukuoka, H. *Proc. Fullerene Symp.* (in Japanese) **1998**, *14*, 234.

(7) (a) Roy, S. B.; Sim, K. E.; Caplin, A. D. *Philos. Mag. B* **1992**, *65*, 1445. (b) Smelyansky, V. I.; Tse, J. S. *Chem. Phys. Lett.* **1997**, *264*, 459.

(8) Saito, S.; Oshiyama, A. *Phys. Rev. B* **1995**, *51*, 2628.

(9) (a) Shimizu, F.; Maniwa, Y.; Kume, K.; Kawaji, H.; Yamanaka, S.; Ishikawa, M. *Phys. Rev. B* **1996**, *54*, 13242. (b) Shimizu, F.; Maniwa, Y.; Kume, K.; Kawaji, H.; Yamanaka, S.; Ishikawa, M. *Synth. Met.* **1997**, *86*, 2141.

(10) (a) Evers, J.; Oehlinger, G.; Ott, H. R. *J. Less-Common Met.* **1980**, *69*, 389. (b) Imai, M.; Hirata, K.; Hirano, T. *Physica C* **1995**, *245*, 12.

(11) (a) Yin, M. T.; Cohen, M. L. *Phys. Rev. B* **1982**, *26*, 5668. (b) Chang, K. J.; Dacorogna, M. M.; Cohen, M. L.; Mignot, J. M.; Chouteau, G.; Martinez, G. *Phys. Rev. Lett.* **1985**, *54*, 2375. (c) Martinez, G.; Mignot, J. M.; Chouteau, G.; Chang, K. J.; Dacorogna, M. M.; Cohen, M. L. *Phys. Scr.* **1986**, *13*, 226. (d) Needs, R. J.; Mujica, A. *Phys. Rev. B* **1995**, *51*, 9652.

(12) (a) Hebard, A. F.; Rosseinsky, M. J.; Haddon, R. C.; Murphy, D. W.; Glarum, S. H.; Palstra, T. T. M.; Ramirez, A. P.; Kortan, A. R. *Nature* **1991**, *350*, 600. (b) Rosseinsky, M. J.; Ramirez, A. P.; Glarum, S. H.; Murphy, D. W.; Haddon, R. C.; Hebard, A. F.; Palstra, T. T. M.; Kortan, A. R.; Zahurak, S. M.; Makhija, A. V. *Phys. Rev. Lett.* **1991**, *66*, 2830. (c) Holczer, K.; Klein, O.; Huang, S.-M.; Kaner, R. B.; Fu, K.-J.; Whetten, R. L.; Diederich, F. *Science* **1991**, *252*, 1154. (d) Tanigaki, K.; Ebbesen, T. W.; Saito, S.; Mizuki, J.; Tsai, J. S.; Kubo, Y.; Kuroshima, S. *Nature* **1991**, *352*, 222. (e) Kelty, S. P.; Chen, C.-C.; Lieber, C. M. *Nature* **1991**, *352*, 223. (f) Kortan, A. R.; Kopylov, N.; Glarum, S.; Gyorgy, E. M.; Ramirez, A. P.; Fleming, R. M.; Thiel, F. A.; Haddon, R. C. *Nature* **1992**, *355*, 529. (g) Kortan, A. R.; Kopylov, N.; Glarum, S.; Gyorgy, E. M.; Ramirez, A. P.; Fleming, R. M.; Zhou, O.; Thiel, F. A.; Trevor, P. L.; Haddon, R. C. *Nature* **1992**, *360*, 566.

(13) (a) Jahn, H. A.; Teller, E. *Proc. R. Soc. London, Ser. A* **1937**, *161*, 220. (b) Ceulemans, A.; Vanquickenborne, L. G. *Structure and Bonding*; Springer: Berlin, Heidelberg, 1989; Vol. 71.

(14) Koga, N.; Morokuma, K. *Chem. Phys. Lett.* **1992**, *196*, 191.

(15) (a) Varma, C. M.; Zaanen, J.; Raghavachari, K. *Science* **1991**, *254*, 989. (b) Lannoo, M.; Baraff, G. A.; Schlüter, M.; Tomanek, D. *Phys. Rev. B* **1991**, *44*, 12106. (c) Zhang, F. C.; Ogata, M.; Rice, T. M. *Phys. Rev. Lett.* **1991**, *67*, 3452. (d) Johnson, K. H.; McHenry, M. E.; Clougherty, D. P. *Physica C* **1991**, *183*, 319. (e) Schlüter, M.; Lannoo, M.; Needels, M.; Baraff, G. A.; Tomanek, D. *Phys. Rev. Lett.* **1992**, *68*, 526. (f) Asai, Y.; Kawaguchi, Y. *Phys. Rev. B* **1992**, *46*, 1265. (g) Faulhaber, J. C. R.; Ko, D. Y. K.; Briddon, P. R. *Phys. Rev. B* **1993**, *48*, 661.

(16) Yoshizawa, K.; Kato, T.; Yamabe, T. *J. Chem. Phys.* **1998**, *109*, in press.

(17) Stewart, J. J. P. *J. Comput. Chem.* **1989**, *10*, 209, 221.

(18) Grimvall, G. *The Electron-Phonon Interaction in Metals*; North-Holland: Amsterdam, 1981.

(19) Fischer, G. *Vibronic Coupling*: *The Interaction between the Electronic and Nuclear Motions*; Academic: London, 1984.

(20) (a) Bersuker, J. B. *The Jahn-Teller Effect and Vibronic Interactions in Modern Chemistry*; Plenum: New York, 1984. (b) Bersuker, J. B.; Polinger, V. Z. *Vibronic Interactions in Molecules and Crystals*; Springer: Berlin, 1989.

(21) Kamimura, H.; Sugano, S.; Tanabe, Y. *Ligand Field Theory and Its Application* (in Japanese); Syokabo: Tokyo, 1969.

(22) Conwell, E. M. *Phys. Rev. B* **1980**, *22*, 1761.

(23) Kholpin, V. P.; Polinger, V. Z.; Bersuker, J. B. *Theor. Chim. Acta* **1978**, *48*, 87.

(24) Frisch, M. J.; Trucks, G. W.; Schlegel, H. B.; Gill, P. M. W.; Johnson, B. G.; Robb, M. A.; Cheeseman, J. R.; Keith, T. A.; Petersson, G. A.; Montgomery, J. A.; Raghavachari, K.; Al-Laham, M. A.; Zakrzewski, V. G.; Ortiz, J. V.; Foresman, J. B.; Cioslowski, J.; Stefanov, B. B.; Nanayakkara, A.; Challacombe, M.; Peng, C. Y.; Ayala, P. Y.; Chen, W.; Wong, M. W.; Andres, J. L.; Replogle, E. S.; Gomperts, R.; Martin, R. L.; Fox, D. J.; Binkley, J. S.; Defrees, D. J.; Baker, J.; Stewart, J. J. P.; Head-Gordon, M.; Gonzalez, C.; Pople, J. A. *Gaussian 94*; Gaussian Inc.: Pittsburgh, PA, 1995.

(25) Silverstein, R. M.; Bassler, G. C.; Morril, T. C. *Spectrometric Identification of Organic Compounds*, 4th ed; Wiley: New York, 1981.

(26) (a) Fang, S. L.; Grigorian, L.; Eklund, P. C.; Dresselhaus, G.; Dresselhaus, M. S.; Kawaji, H.; Yamanaka, S. *Phys. Rev. B* **1998**, *57*, 7686. (b) Guyot, Y.; Champagnon, B.; Reny, E.; Cros, C.; Pouchard, M.; Melinon, P.; Perez, A. *Phys. Rev. B* **1998**, *57*, R9475.

(27) Our PM3 calculations afforded Si−H stretching values of 1909 and 1937 cm^{-1} for silane, SiH_4.

(28) (a) Yoshizawa, K.; Kato, T.; Yamabe, T. *J. Chem. Phys.* **1998**, *108*, 7637. (b) Kato, T.; Yoshizawa, K.; Yamabe, T. *J. Chem. Phys.*, in press.

(29) See for example: Hebard, A. F. *Phys. Today* **1992** (Nov 26).

(30) Gryko, J.; McMillan, P. F.; Sankey, O. F. *Phys. Rev. B* **1996**, *54*, 3037. This work demonstrated that the Na atoms are also important for the increase in the density of states at the Fermi level.